Thermalization and Indications that Anti-flatness measures Magic

J.-W. Chen, Y.-T. Chen, L. Ebner, J. Halimeh, D. Horn, J. Lap, G. Meher, Y. Ting, J. Minar, B. Müller, AS, L. Schmotzer, C. Seidl, S. Waeber, L. Yaffe, X. Yao

- To understand the dynamics of SU(N) thermalization is often mentionned as important physics project demonstrating quantum atvantage. If so, it must have (non-local) magic.
- We focus on high energy heavy ion collisions.
- The difficulties of this physics are rarely fully appreciated.

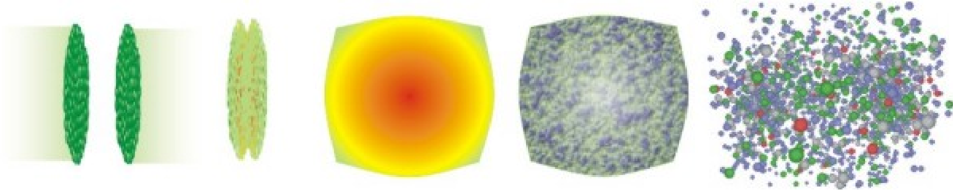

Standard view of HICs, but how can transverse communication happen in less than 1fm/c? $\gamma(Pb) > 2500$ giving it a width of $11\text{fm}/2500 = 0.004\text{fm}$ Transverse fluctuations are large.
arXiv:1605.03954

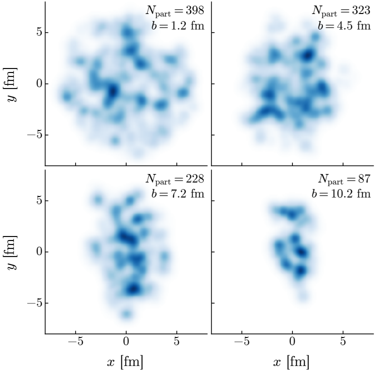

This can be described by holography 1906.05086

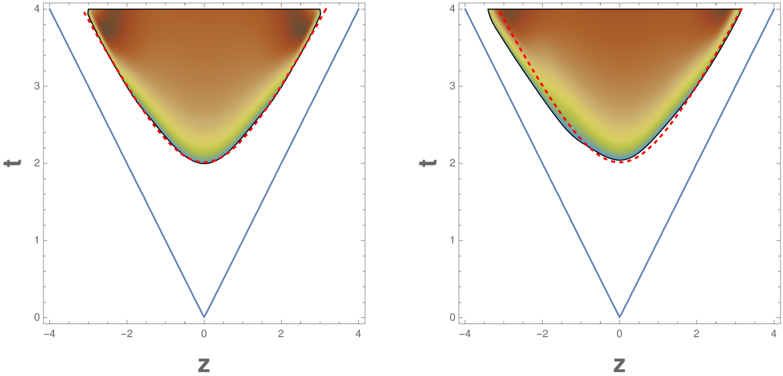

Hydrodynamization occurs at **fixed eigenzeit** $\Rightarrow$ basically not boost dependent, geometric mean

criterium: $\Delta = \frac{1}{p}\sqrt{\delta T^{\mu\nu}\,\delta T_{\mu\nu}} < 0.15$ with $\delta T^{\mu\nu} = T^{\mu\nu} - T^{\mu\nu}_{\text{hydro}}$

Bernhard, Moreland, Bass Liu, Heinz arXiv:1605.03954 Fit result: parameterization of combined entropy density:

$$s \sim \left(\frac{\tilde{T}_A^p + \tilde{T}_B^p}{2}\right)^{1/p} \quad , \quad -\infty \leq p \leq \infty$$

$$\tilde{T}(x_{perp}) = \sum_{i=1}^{N_{part}} \frac{\gamma_i}{2\pi w^2} \exp\left(-\frac{(x_\perp - x_{i,\perp})^2}{2w^2}\right)$$

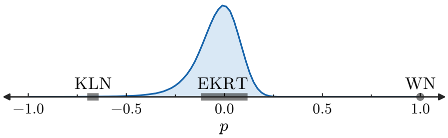

By construction the hydro initialization time must be identical for each transverse pixel. Both features are reproduced by AdS/CFT 1906.05086

There is very much high precision data, e.g. from ALICE.

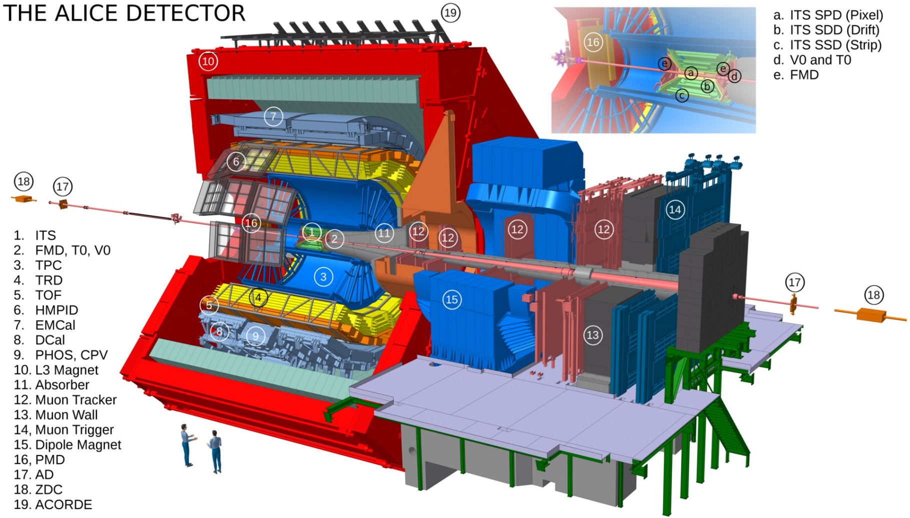

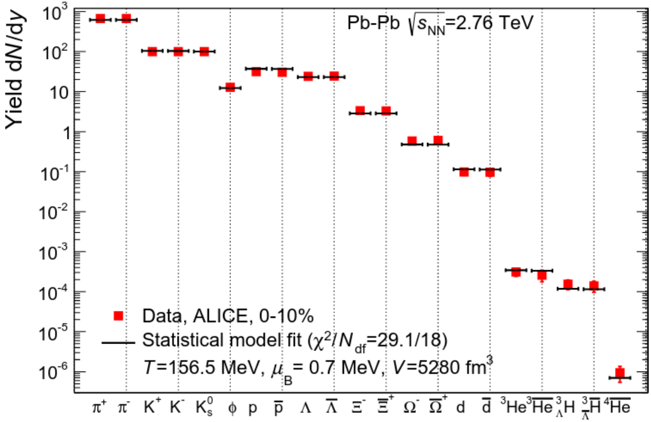

But: R(rms , ${}^3_\Lambda H$)=10.6 fm$\sim 2R_{\mathrm{Pb}}$;

$-B = 0.4\mathrm{MeV} << 156$ MeV the yield should be suppressed

Upshot: Only the combination of all established approaches like QFT, LGT, string theory, QIS, ETH etc. allow to explain all puzzles. E.g. ETH can explain the ${}^{3}_{\Lambda}H$ puzzle and AdS/CFT can explain the pixel and time dilatation puzzles ...

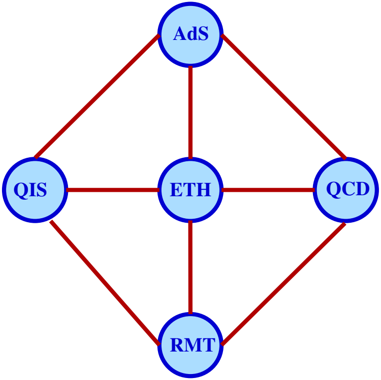

The Eigenstate Thermalization Hypothesis (ETH)

D'Alesio, Kafri, Polkovnikov, Rigol arXiv:1509.06411

$$O_{mn} = \langle m|\hat{O}|n\rangle = O(\bar{E})\delta_{mn} + e^{-S(\bar{E})/2} f_O(\bar{E},\omega) R_{mn}$$

$\bar{E} = (E_m + E_n)/2$, $\omega = (E_m - E_n)$, $S(\bar{E})$ thermodynamic entropy at energy $\bar{E}$, $O(\bar{E})$ and $f_O(\bar{E},\omega)$ are smooth functions, $O(\bar{E})$ is identical to the expectation value of the microcanonical ensemble at energy $\bar{E}$, and R_{mn} is a strongly fluctuating matrix (in the sense of RMT?)

Physics explanation: entropy production, i.e. information loss happens in spite of unitary time evolution because experiments detect only a small amount of information.

Testing ETH for SU(2)

Usually, people use the Kogut-Susskind lattice formulation. We, i.e. M. Hanada et al. argue that the orbifold lattice formulation is more efficient on quantum computers: arXiv:2411.13161

$$\hat{H} = \frac{g^2}{2}\sum_{\text{links}} \hat{E}^2 - \frac{1}{2g^2}\sum_{\Box}\left(\hat{\Box} + \hat{\Box}^\dagger\right)$$

$$\hat{\Box} = \sum_{\alpha,\beta,\gamma,\delta=\frac{1}{2}}^{\frac{1}{2}} \hat{U}_{\alpha\beta}\hat{U}_{\beta\gamma}\hat{U}_{\gamma\delta}\hat{U}_{\delta\alpha} \quad .$$

Does SU(2) in e.g. 1+2 dimension show ETH behaviour? It can be simulated on classical computers, expressing it by spin couplings

N. Klco, J. R. Stryker and M. J. Savage, arXiv:1803.03326

In 1+2 dimensions

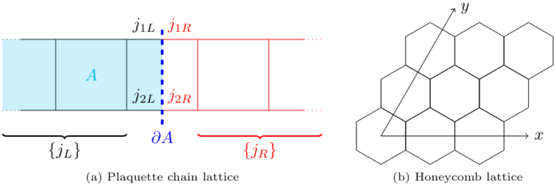

(a) Plaquette chain lattice (b) Honeycomb lattice

In 1+3 dimensions: Kavaki and Lewis arXiv:2401.14570

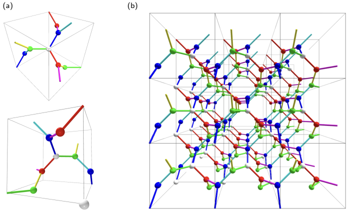

Gauss law is automatically fulfilled; Many thanks go to Erlangen National High Performance Computing Center

$$
\begin{aligned}
&\langle \chi_{\dots,j_\ell^{t,b},q_{\ell f},j_{af}^{t,b},q_{rf},j_r^{t,b},\dots} | \hat{\Box} | \chi_{\dots,j_\ell^{t,b},q_{\ell i},j_{ai}^{t,b},q_{ri},j_r^{t,b},\dots} \rangle = \\
&\sqrt{\dim(j_{ai}^t)\dim(j_{af}^t)\dim(j_{ai}^b)\dim(j_{af}^b)} \\
&\times \sqrt{\dim(q_{\ell i})\dim(q_{\ell f})\dim(q_{ri})\dim(q_{rf})} \\
&\times (-1)^{j_\ell^t + j_\ell^b + j_r^t + j_r^b + 2(j_{af}^t + j_{af}^b - q_{\ell i} - q_{ri})} \\
&\times \begin{Bmatrix} j_\ell^t & j_{ai}^t & q_{\ell i} \\ \frac{1}{2} & q_{\ell f} & j_{af}^t \end{Bmatrix} \begin{Bmatrix} j_\ell^b & j_{ai}^b & q_{\ell i} \\ \frac{1}{2} & q_{\ell f} & j_{af}^b \end{Bmatrix} \begin{Bmatrix} j_r^t & j_{ai}^t & q_{ri} \\ \frac{1}{2} & q_{rf} & j_{af}^t \end{Bmatrix} \begin{Bmatrix} j_r^b & j_{ai}^b & q_{ri} \\ \frac{1}{2} & q_{rf} & j_{af}^b \end{Bmatrix}
\end{aligned}
$$

We construct up to 10^5 states.

The restricted gap ratio $r = \frac{\min[\delta_\alpha, \delta_{\alpha-1}]}{\max[\delta_\alpha, \delta_{\alpha-1}]}$ $\delta_\alpha = E_{\alpha+1} - E_\alpha$

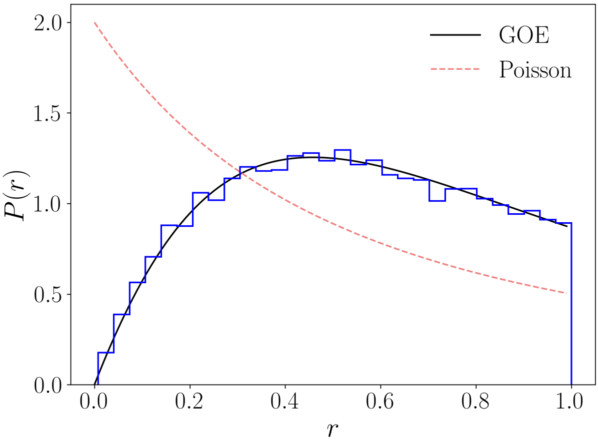

g^2 dependence of the averaged restricted gap ratio $\langle r \rangle$. GOE predicts 0.53, Poisson predicts 0.39.

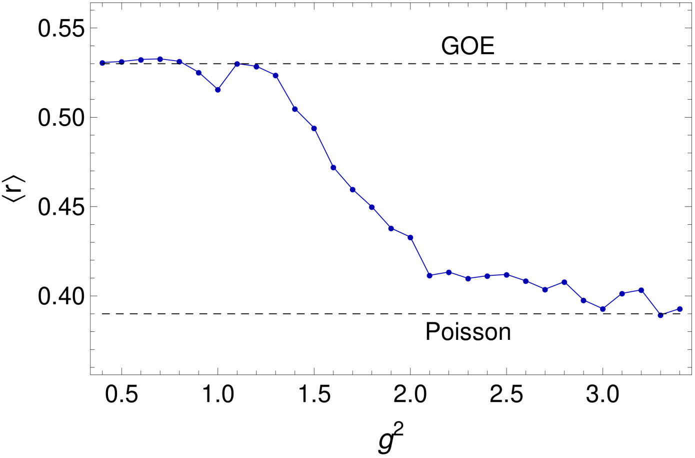

Test of $j_{\max}$ convergence.

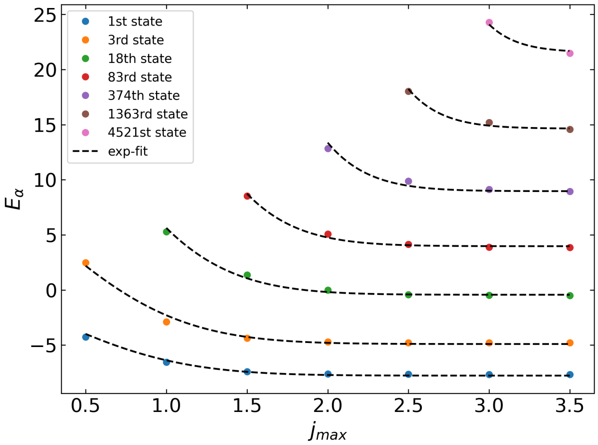

The Page curve for a chain of 17 plaquettes 2401.15184

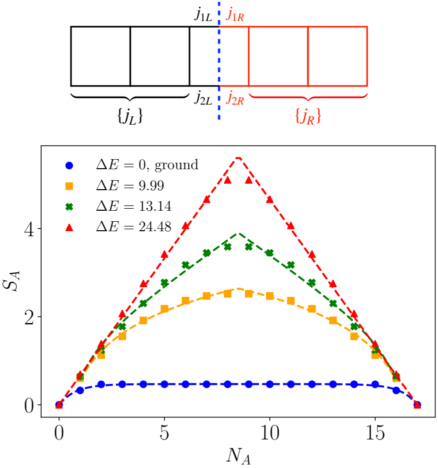

$$S_A = -\mathrm{Tr}\Big(\rho_A \ln(\rho_A)\Big) \quad ; \quad \rho_A = \mathrm{Tr}_{A^c}\,\rho \quad ; \quad \rho_{A,th}(\beta) = \mathrm{Tr}_{A^c}\left(e^{-\beta H}\right)/\mathrm{Tr}\,e^{-\beta H}$$

Real time evolution of entanglement entropy

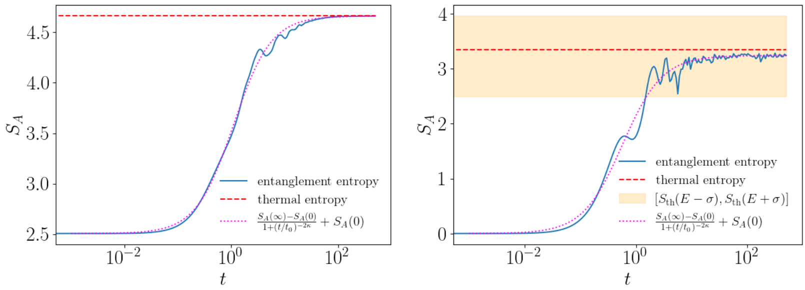

We fit with the function

$$S_A(t) = S_A(0) + \frac{S_A(\infty) - S_A(0)}{1 + (t/t_0)^{-2\kappa}}$$

$\kappa = 0.616 \pm 0.003$, $\log t_0 = 0.097 \pm 0.004$ close to the mean energy
$\kappa = 0.608 \pm 0.014$, $\log t_0 = -0.555 \pm 0.021$ ground state of subsystem
($N_A = 3$, $ag^2 = 1.2$ $j_{\rm max} = 1$)

Anti-flatness ≤ Magic

$$M_A = \frac{\mathrm{Tr}(\rho_A^3)}{[\mathrm{Tr}(\rho_A^2)]^2} - 1$$

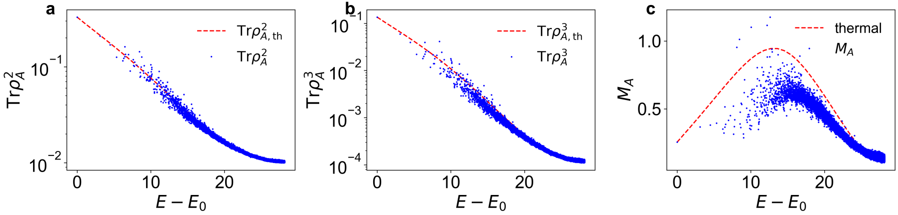

Anti-flatness spectrum for a small subsystem. The blue dots show
(a) $\mathrm{Tr}\rho_A^2$,
(b) $\mathrm{Tr}\rho_A^3$,
(c) the anti-flatness of the entanglement spectrum M_A of all energy eigenstates below the spectral peak; $j_{\mathrm{max}} = 1$, $ag^2 = 1.2$, $N_A = 3$.

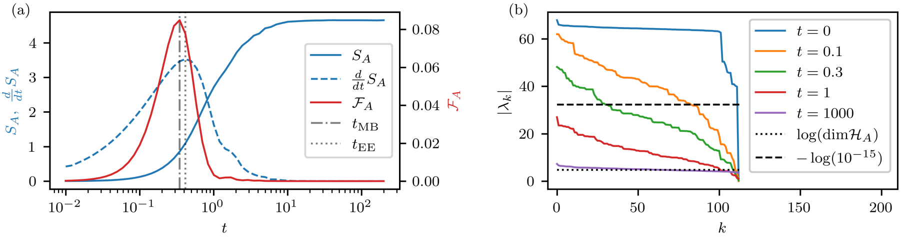

(a) Real-time evolution of entanglement entropy S_A (blue solid line, left scale) and anti-flatness $\mathcal{F}_A$ (red solid line, right scale) of a small two-plaquette subsystem in the middle of an aperiodic seven-plaquette chain with $j_{\mathrm{max}} = 1$, ergodic coupling $g^2 = 1$ and asymmetric boundary conditions $\{j_{\mathrm{ext}}\} = \{0, 0, 0, 1\}$ for a randomly chosen, highly excited initial electric basis state with energy $E - E_0 \approx 19.17$. The blue dashed line shows the entanglement entropy growth rate. t_{MB} and t_{EE}, indicated by gray lines, correspond to the time of the magic barrier and maximum entanglement growth rate, respectively. (b) Entanglement spectra of the above state at different times during the thermalization process. λ_k denotes the k-th eigenvalue of the entanglement Hamiltonian $H_A = -\log\rho_A$. The flat-spectrum limit is given by $|\lambda_k| = \log(\dim(\mathcal{H}_A)) \approx 4.727$.

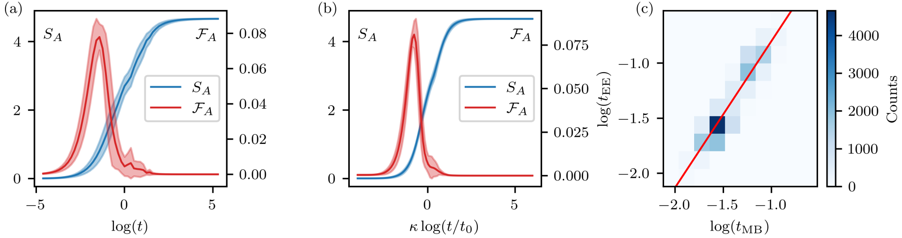

a) Real-time evolution of S_A and $\mathcal{F}_A$ for a small two-plaquette subsystem in the middle of an aperiodic seven-plaquette chain with $j_{\max} = 1$ and asymmetric boundary conditions $\{j_{\text{ext}}\} = \{0, 0, 0, 1\}$ at ergodic coupling $g^2 = 1$ for all electric basis states within the highly excited energy window $E - E_0 \in [19.71, 20.21]$. The energy window contains 2728 states. (b) Rescaled time evolution of the same system and state ensemble. The real time t is replaced by $\kappa \log(t/t_0)$ with state-dependent fit parameters κ and t_0, such that the thermalization of different states is synchronized. The solid lines and bands in (a) and (b) are the ensemble means and 1σ-bands. The left and right scales correspond to S_A and $\mathcal{F}_A$, respectively. (c) 2D histogram showing the joint distribution of magic barrier time t_{MB} and time of maximum entanglement entropy growth t_{EE} on logarithmic scales for all 18389 physical electric basis states of the above system with energies below the spectrum mean. Color intensity corresponds to bin counts. The red line represents a linear fit with slope 1.331 and intercept 0.530.

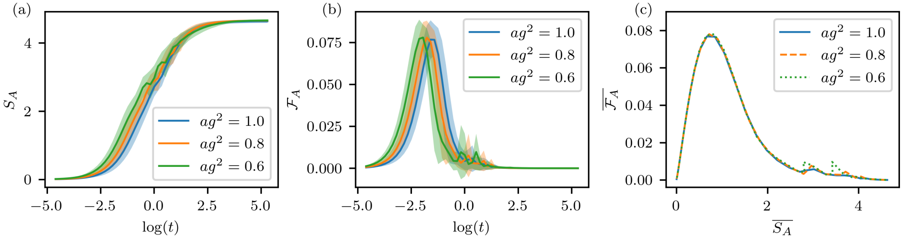

Coupling dependence of entanglement dynamics. Real-time evolution of (a) S_A and (b) $\mathcal{F}_A$ for a small two-plaquette subsystem in the middle of an aperiodic seven-plaquette chain with $j_{\mathrm{max}} = 1$ and asymmetric boundary conditions $\{j_{\mathrm{ext}}\} = \{0, 0, 0, 1\}$ at different ergodic couplings $g^2 \in \{1.0, 0.8, 0.6\}$. The ensemble of electric basis states is chosen such that at $g^2 = 0.6$ they lie in the highly excited energy window $E - E_0 \in [26.48, 26.98]$. This ensemble contains 2995 states. The solid lines and bands in (a) and (b) are the ensemble means and 1σ-bands. (c) Relations between the ensemble means $\overline{S}_A$ an $\overline{\mathcal{F}}_A$ for different ergodic couplings, which exhibit very mild coupling dependence.

The theoretical description of thermalization of SU(2) gauge theory requires indeed Magic, i.e. quantum computing, as expected.

But can one take the full complexity of physical HICs into account, e.g. hadronization?

quark-gluon entanglement ⇒ hadron entanglement

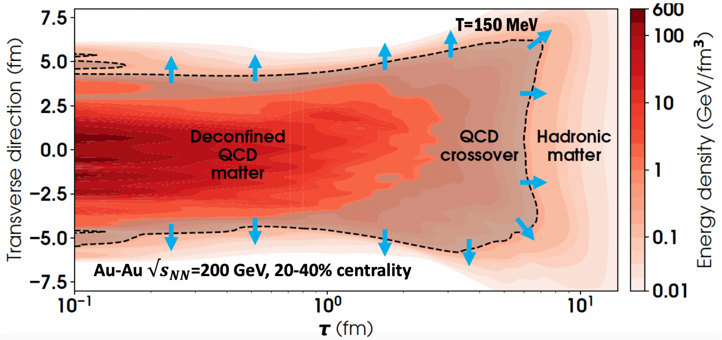

A 1+1 dimensional toy model: Ebner et al. 2605.28939

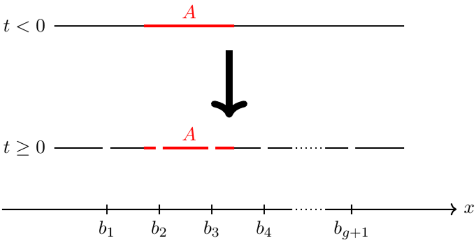

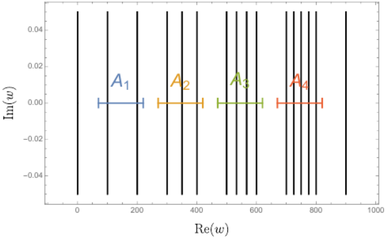

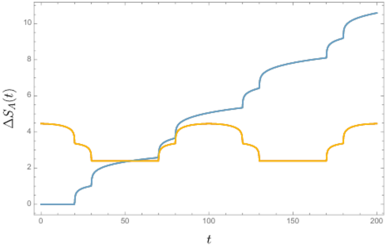

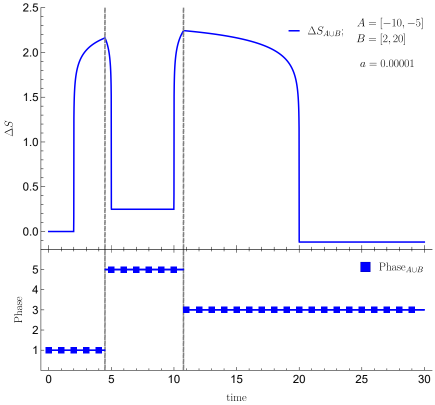

To describe the entanglement entropy for one interval Cardy and Calabrese introduced a quasi particle picture arXiv:cond-mat/0503393. However, this fails to accurately describe the entanglement entropy for multiple intervals and thus, the mutual information. C. T. Asplund and A. Bernamonti, arXiv:1311.4173

Example: Entanglement entropy, one splitting quench, two disjoint subsystems (A,B), $\Delta S = S(t) - S_0$; S_0 before quench

C. T. Asplund and A. Bernamonti, arXiv:1311.4173

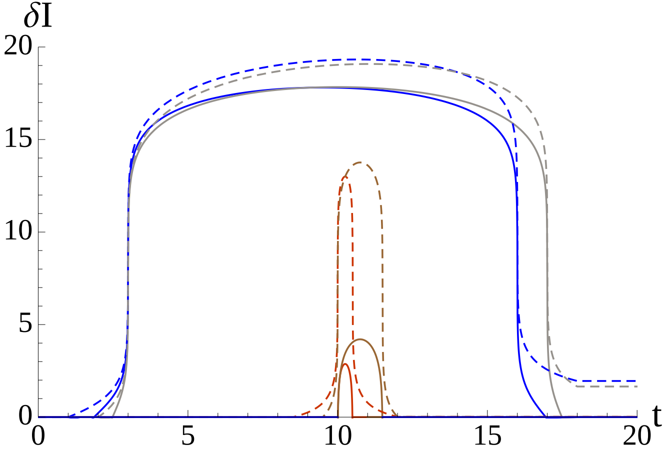

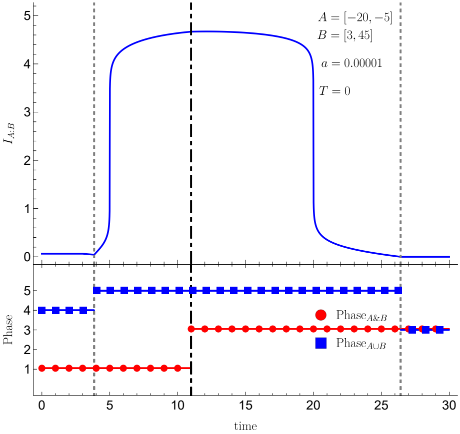

Our mutual information with DQPTs $I(A:B) := S_A + S_B - S_{A\cup B}$

- Conformal symmetry allows to map all single-boundary quenched (split or join) worldsheets onto the UHP.
- Holographically this is described by introducing an end-of-the-world brane Q and the Gibbons-Hawking-York action (Takayanagi, Fujita, Tonni)
  $I_E = \frac{-1}{16\pi G_N} \int_N \sqrt{g}(R - 2\Lambda) - \frac{1}{8\pi G_N} \int_Q \sqrt{h}(K - T)$
- The entanglement entropy for the vacuum without a quench is time independent (static). The entanglement entropy for a quenched worldsheet is time dependent (both in Euclidean, τ, and Lorentz time, t, called dynamical)
- There are many different choices for geodesics (RT proposal). The one with the smallest action/shortest length contributes, resulting in phase transitions, DQPTs or QPTs. The phases for two intervals, i.e., four points z_1, z_2, z_3, z_4 are best parameterized by (conformally invariant) cross-ratios.
  holographically: $v_{ij} = \frac{|z_i - z_j||\bar{z}_i - \bar{z}_j|}{|z_i - \bar{z}_i||z_j - \bar{z}_j|}$
  on the lattice: $v_{ij} = \frac{\sin^2[\pi(w_i - w_j)/2N]}{|\sin(\pi w_i/N)\sin(\pi w_j/N)|}$

possible geodesic configurations (phases) in the RT proposal

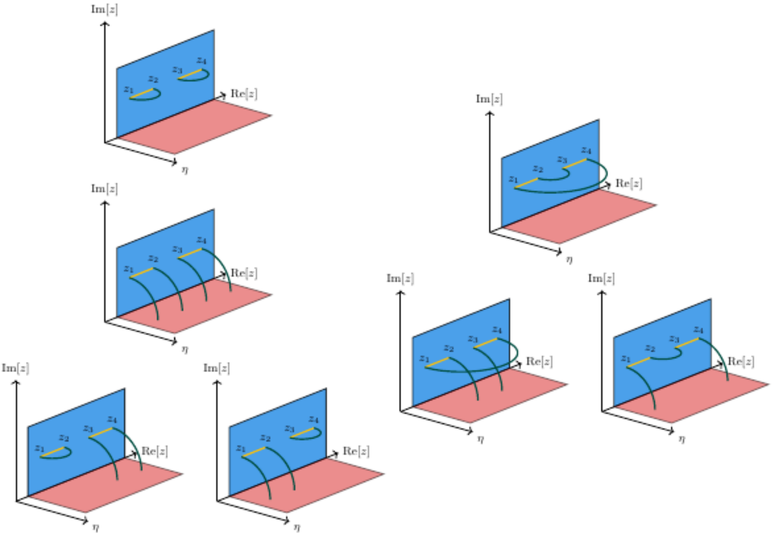

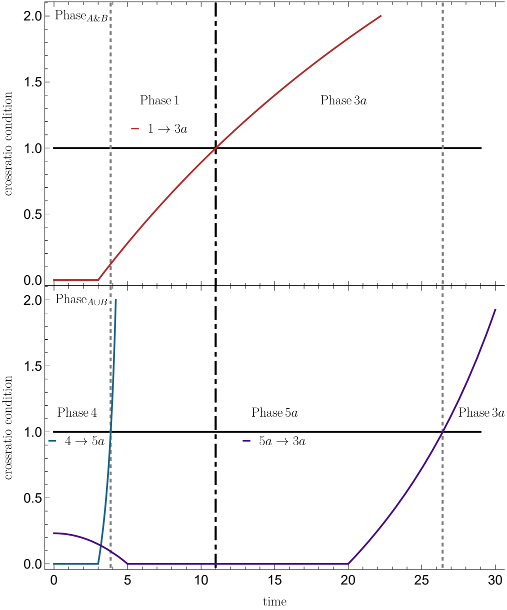

Phase transitions for mutual information (one split)

A very pleasant surprise

Holography is valid for $c = \infty$ while our lattice calculations are done for $c = 1$. There is no good reason why the results should agree.

but they do!

Perhaps this could provide a hint for why holographic methods work.

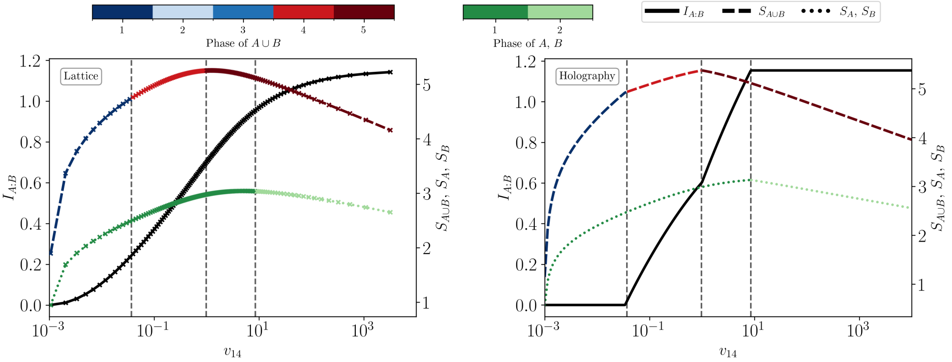

Static mutual information and entanglement entropies for two intervals on a strip. Left: Free-fermion lattice result (4000 sites, open boundary conditions, $c = 1$). Right: Holographic result for $c = \infty$.

Conclusions

- Thermalization in HICs requires quantum computing. (QCD is time-reversal invariant, i.e. entanglement information does not get lost)
- ETH, decoherence and thermalization of isolated quantum systems are topics of universal interest, HICs are perfect isolated systems.
- We observe an antiflatness (Magic) peak synchronized with entropy growth.
- The complete problem is intimidating. We found a rich network of DQPT for mutual information
- Generalization to many quenches? arXiv:2412.01808

Backup

a first try in quantum computing J.-W. Chen, Y.-T. Chen, G. Meher, X,Yao, BM,AS, arXiv:2603.23948

Disclaimer: I am a complete greenhorn, who just tries to profit from an opportunity to learn some basics about quantum computing. My aim is to motivate some expert to look into this.

On a plaquette chain the Hilbert space of singlet SU(2) Kogut-Susskind states can be mapped onto a 1d spin model N. Klco, J.R. Stryker, M.J. Savage arXiv:1908.06935.

A quantum circuit generated with QISKIT

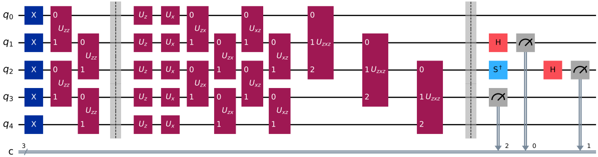

What is anti-flatness?

1.) Gottesman-Knill theorem: Clifford gates (e.g. Hadamar, Phase and CNOT gate) generate entanglement (Cliford orbits) but can be efficiently implemented with classical resources (no universal gate set).

$$H = \frac{1}{\sqrt{2}}\begin{pmatrix} 1 & 1 \\ 1 & -1 \end{pmatrix}; \quad S = \begin{pmatrix} 1 & 0 \\ 0 & e^{i\pi/2} \end{pmatrix}; \quad CNOT = \begin{pmatrix} 1 & 0 & 0 & 0 \\ 0 & 1 & 0 & 0 \\ 0 & 0 & 0 & 1 \\ 0 & 0 & 1 & 0 \end{pmatrix}$$

2.) Li and Haldane: The reduced density matrix gives entanglement entropy, the spectrum of the reduced density matrix contains additional information. One needs a non-flat spectrum of eigenvalues.

$$\rho_A = e^{-H}$$

with “Hamiltonian” H and “time” 1

One has to add e.g. T gates to get a universal gate set and thus be able to achieve quantum advantage

$$T = \begin{pmatrix} 1 & 0 \\ 0 & e^{i\pi/4} \end{pmatrix}$$

Cao et al. 2403.07056 have shown anti-flatness $\leq$ Magic

The free fermion Hamiltonian is the low-energy limit of the nearest-neighbor hopping Hamiltonian

$$H = -\gamma \sum_{i=i_1}^{i_N} \left(c_i^\dagger c_{i+1} + c_{i+1}^\dagger c_i \right)$$